The variable effect of clouds on atmospheric absorption of solar radiation

Zhanqing Li*, Howard W. Barker† & Louis Moreau‡

* Canada Centre for Remote Sensing, 588 Booth Street, Ottawa, Ontario K1V 0J6, Canada
† Atmospheric Environment Service, Downsview, Ontario, Canada
‡ Intera Information Technologies Corporation, Ottawa, Ontario, Canada

A four-year global record of solar flux observed from both space and the Earth's surface allows an examination of the effect of clouds on the atmospheric absorption of solar radiation. The results indicate that, contrary to some recent suggestions, the effect of clouds is highly variable and present general circulation models should be able to incorporate cloud absorption into climate simulations.

VARIABLE absorption of solar energy by the Earth's surface and atmosphere is the driving force behind climate and is modulated primarily by clouds. Cloud–radiation interactions are among the most important yet least understood processes controlling climate[1]. This seriously hinders general circulation model (GCM) predictions of climate change. A more fundamental concern, however, is that after more than 40 years of work[2], both theory and observation of the absorption of solar radiation by clouds are still fraught with uncertainties. In essence, cloud absorption inferred from aircraft measurements of solar radiation often exceeds model calculations. Such a discrepancy is referred to as the 'cloud absorption anomaly'. As yet, it is not clear whether this phenomenon is real or an aberration stemming from uncertainties in either aircraft flux observations or input parameters for radiative-transfer modelling[3].

Recent studies[4–6] suggest that the cloud absorption anomaly is not only real but much larger than implied by previous work. These studies employed space-borne, airborne and ground-based observations to infer the effect of clouds on atmospheric absorption of solar radiation by determining the ratio, R, of the short-wavelength cloud radiative forcing (CRF) at the Earth's surface to that at the top of the atmosphere (TOA). They found R to be consistently about 1.5, whereas conventional radiative-transfer models tend to produce R values of about 1.0 (ref. 4). In order for radiative-transfer models to produce $R = 1.5$, the specific absorption of cloud droplets would need to be increased uniformly in the near-infrared by a factor of 40 relative to conventional values[7]. If R has a value of 1.5 globally, contemporary radiation models would need to be able to increase their absorption of radiation by cloud particles by $\sim 25\ \mathrm{W\ m^{-2}}$, on average. In separate studies[8,9], it has been demonstrated that such models also underestimate absorption of radiation by clear skies by a similar amount. Taking these findings together implies that the radiation budgets of the atmosphere and surface could differ from those computed by GCMs by up to a factor of two, thus seriously affecting their simulations of the Earth's current climate and their predictions of climate change due to, for example, increasing amounts of greenhouse gases.

Here we determine R following the same methodologies as refs 4 and 5, but using different data sets of longer duration and broader coverage. We find that R is highly variable in the tropics with a median of about 1.4, less variable at mid-latitudes with a median of about 1.1, and consistently less than 1.0 in polar regions. We propose that large values and high variations of R may be related to the presence of absorbing aerosols and the uncertainties in both the observed and inferred solar flux data used here. Therefore, a substantial revision of our understanding of cloud absorption and its impact on the atmosphere's energy budget[4] may not, after all, prove to be necessary if the effects of absorbing aerosols are properly incorporated.

Determination of cloud effects

The ratio R is defined as

$$R = \frac{\mathrm{CRF_{SFC}}}{\mathrm{CRF_{TOA}}} = \frac{F^{\mathrm{all}}_{\mathrm{SFC}} - F^{\mathrm{clr}}_{\mathrm{SFC}}}{F^{\mathrm{all}}_{\mathrm{TOA}} - F^{\mathrm{clr}}_{\mathrm{TOA}}} \quad (1)$$

where $\mathrm{CRF_{SFC}}$ and $\mathrm{CRF_{TOA}}$ denote CRF at the surface (SFC) and the TOA, respectively. $\mathrm{CRF_{SFC}}$ and $\mathrm{CRF_{TOA}}$ are defined as differences between net solar radiative fluxes F for all-sky (clear and cloudy skies) and clear-sky conditions indicated by the superscripts. Because it is impossible, in practice, to have simultaneous clear and cloudy measurements, mean clear-sky fluxes were based on available cloudless events over an averaging period. The resulting fluxes are assumed to represent those that would be observed should clear skies occur constantly. This simplification was shown to be a minor problem for monthly-mean solar radiation[10,11]. As

$$\mathrm{CRF_{SFC}} = \mathrm{CRF_{TOA}} - \mathrm{CRF_{ATM}} \quad (2)$$

where $\mathrm{CRF_{ATM}}$ is atmospheric CRF, then

$$\mathrm{CRF_{ATM}} = (1 - R)\mathrm{CRF_{TOA}} \quad (3)$$

In general, $\mathrm{CRF_{TOA}} < 0$ (ref. 12), and so $R > 1$ and $R < 1$ imply, respectively, that clouds enhance and reduce atmospheric absorption relative to clear-sky absorption. The case $R = 1$ is when cloud absorption exactly equals the reduction in absorption by gases and aerosols beneath cloud due to reduced transmittance of incoming radiation, less the slight enhancement in absorption by gases and aerosols above cloud due to increased reflectance.

Using the definition in equation (1), Ramanathan *et al.*[5] obtained R for the western equatorial Pacific Ocean. In their study, all-sky and clear-sky TOA fluxes were taken from satellite measurements. All-sky surface net fluxes were determined as the residual term in the surface heat-balance equation, and clear-sky surface net fluxes were inferred from satellite-based clear-sky TOA fluxes using an inversion algorithm[13]. Cess *et al.*[4] obtained R from the slope, s, of the linear regression between coincidental TOA albedo and atmospheric transmittance of solar radiation R and s are related by

$$R = -\frac{(1 - \alpha_{\mathrm{SFC}})}{s} \quad (4)$$

where α_{SFC} denotes surface albedo. (Note that the sign of s in equation is opposite to that used in ref. 4.) The advantage of using s instead of R is that there are more observations of surface insolation than surface net solar flux and that estimation of surface albedo is avoided. The disadvantage, however, is that determination of s requires multiple pairs of coincident observations obtained over a period, or area, in order to perform a reliable regression analysis. This will limit the ability to analyse

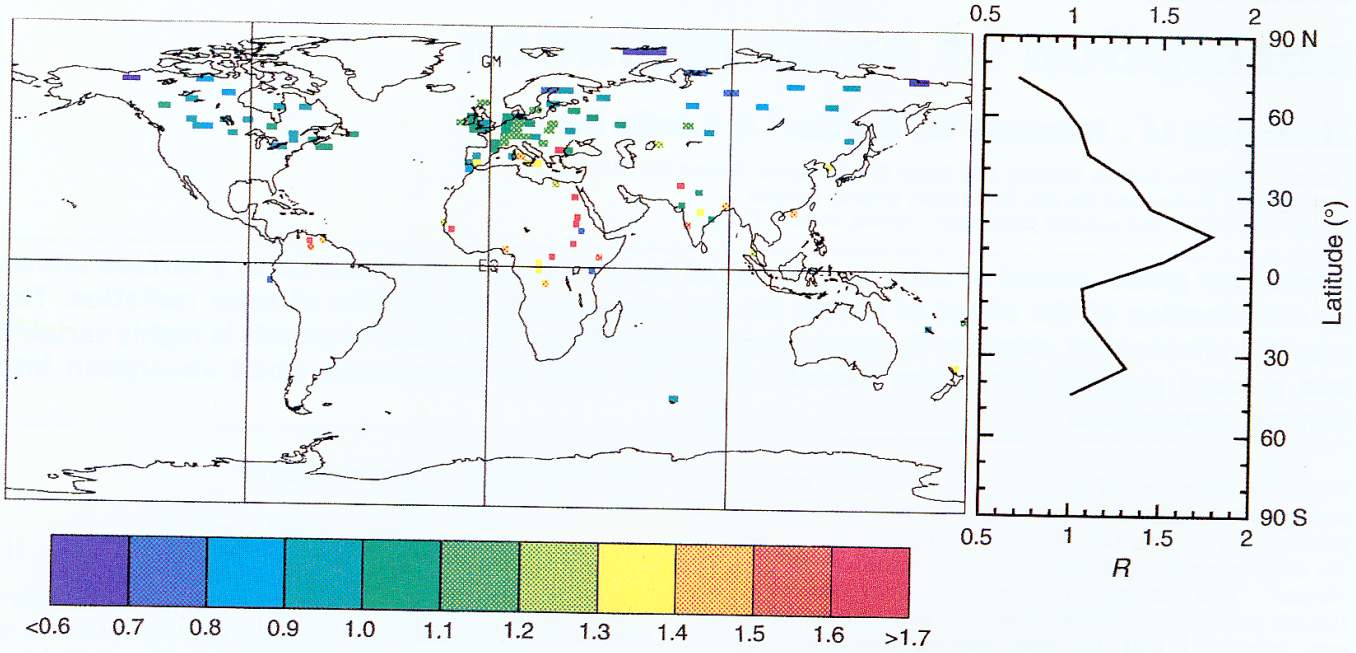

FIG. 1 Left, global distribution of R, the ratio of mean short-wavelength cloud radiative forcing (CRF) at the surface to that at the top of the atmosphere (TOA) averaged over the entire data period. Right, the corresponding zonal variation of R.

spatial and temporal variations of R. By analysing co-located satellite and surface measurements at various sites, Cess *et al.*[4] found that values of s are always close to 0.6, whereas GCMs produce values near 0.8. These values of s are approximately equivalent to R of 1.4 and 1.0, respectively[4].

Both the direct (equation (1)) and the regression methods for determining R were employed in this study. To guide the analyses of the observational results, the sensitivity of R to various factors was examined using a conventional radiative-transfer model[13]. Table 1 lists model-generated diurnal-mean values of R calculated from integration of instantaneous clear and cloudy solar fluxes. Although cloud optical depth was held constant at 40 for the calculations of Table 1, sensitivity tests showed that R is almost insensitive to this variable. The dependence of R on solar zenith angle is shown in ref. 7. R decreases significantly with increasing solar zenith angle, cloud-top altitude and surface albedo. A weaker dependence was found on cloud type that was differentiated here by cloud droplet sizes only[14]. It appears from Table 1 that although R depends on a variety of parameters, it rarely exceeds 1.2. These results are for particular profiles of water vapour and aerosols. The results are subject to changes in these profiles. Nevertheless, the maximum diurnal mean value of R never exceeds 1.2 for the combination of typical surface and atmospheric conditions unless there is heavy loading of strongly absorbing aerosol.

Observational data

In our analysis, we used global, monthly-mean measurements from the Earth Radiation Budget Experiment (ERBE)[15] and the Global Energy Balance Archive (GEBA)[16]. (ERBE was a three-satellite programme designed to monitor TOA radiative fluxes, while GEBA processed and archived global surface heat-flux measurements.) Gridded monthly-mean ERBE and GEBA data for cells of 280×280 km^2 were extracted from data sets covering the 46 months from March 1985 to December 1988[17]. Variable record lengths and the effect of quality control results in number of months per cell varying from fewer than 5 at high latitudes to more than 40 in Germany. Both clear-sky and all-sky TOA net solar fluxes were obtained from ERBE measurements. Surface all-sky downwelling solar irradiances were observed by pyranometers deployed in the world-wide radiation network. The accuracy of most pyranometers is estimated to be better than 15 W m^{-2} (ref. 16). Surface all-sky albedos and clear-sky net fluxes were inferred from ERBE using the algorithms in refs 18 and 13, respectively. The latter algorithm has been validated for various regions[5,19]; the former has been shown to give values of clear-sky surface albedo that compare well with an independent algorithm[20].

Temporal and spatial differences between satellite and surface measurements give rise to match-up errors. Errors due to time differences are small, as ERBE provides measurements at various local times and the surface data were taken throughout the day. Spatial match-up errors are much reduced by time averaging. The errors that remain depend on the number of surface stations per cell. It has been shown[21] that match-up errors for monthly data are approximately equal to $24.2/N$ (W m^{-2}) where N is the number of stations per cell; in our study, N ranged from 1 to 10. All matched pairs of satellite and surface data were used except those corresponding to snow-covered land and frozen water which were identified by clear-sky TOA albedos exceeding 0.3. These pairs were excluded for two reasons. First, as seen in Table 1, values of R for bright surfaces differ much from other surfaces. Therefore, the analysis was confined to relatively dark surfaces so that variations in R could be interpreted as changes in atmospheric absorption. Second, ERBE clear-sky identification over snow and ice surfaces is known to be unreliable. After screening, R was computed for each cell on an individual monthly basis; R was also computed for larger time and space domains using the corresponding domain mean values of CRF.

Variability in cloud effects

Figure 1 shows the geographical distribution and latitudinal variation of R computed from mean CRF averaged over the entire data period for every grid. The most striking feature is that R exhibits strong meridional variability. In tropical regions, R is significantly larger than unity and is in apparent agreement with

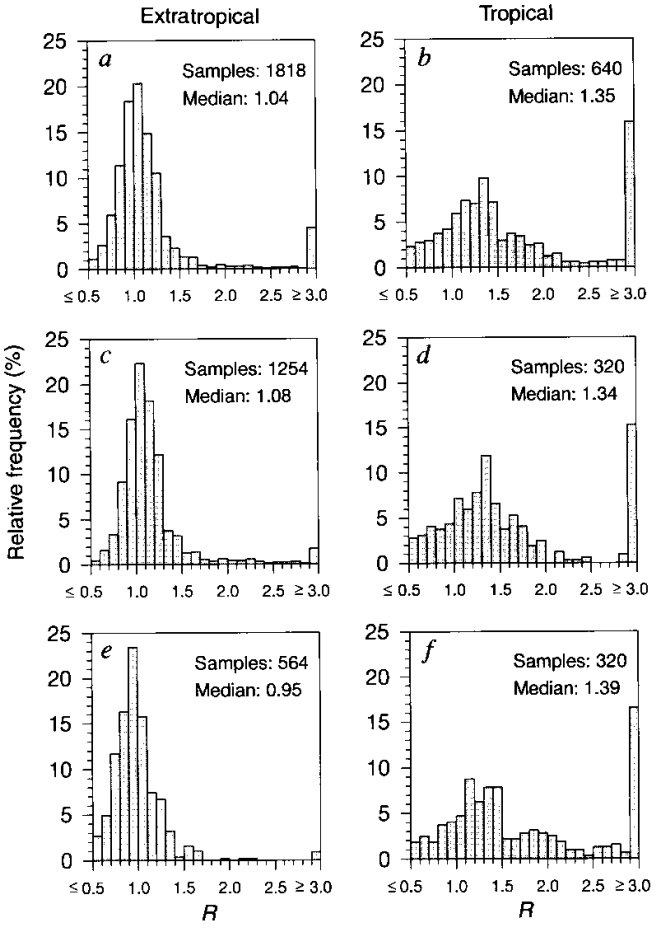

FIG. 2 Relative frequency histograms of monthly R for the tropics (latitude <30°) and extratropics (latitude >30°) using data from: *a* and *b*, all available months; *c* and *d*, April to September inclusive; *e* and *f*, October to March inclusive. Listed on the plots are number of samples and median values of R.

refs 4–6, implying that tropical clouds enhance atmospheric absorption substantially. For mid-latitudes, R is generally between 1.0 and 1.2, implying that clouds slightly increase total atmospheric absorption. In polar regions, R is less than 1, indicating that polar clouds tend to reduce atmospheric absorption compared to clear-sky absorption. It is likely that these gross variations of R are associated with cloud structure and solar zenith angle. However, it should be pointed out that the tropical GEBA sites are primarily in continental regions close to the sources of strong absorbing aerosols produced by biomass burning[22–24], which are, at least, partially responsible for enhanced absorption in the tropics. Unfortunately, lack of such aerosol data on the same time and space scales prevents determining their effects quantitatively. The effect is also manifest in longitudinal variations of R in the mid-latitudes where R is greatest over Europe, intermediate over eastern Canada, and least in central Canada: this pattern corresponds approximately with anthropogenic aerosol loadings[25]. For western Europe, the largest values of R occur near Hamburg and the Rhine Valley which are known to be heavily polluted regions[26]. Conversely, cells with the smallest values of R are near southern Spain and Ireland which are relatively non-polluted.

The data were then sub-divided into two regions, tropics (latitudes ≤30°) and extratropics (latitudes >30°); they were also divided into three time periods, summer (April–September), winter (October–March) and annual (all months). Figure 2 shows relative frequency histograms of R for individual months and cells for each of the six categories. The most striking feature of Fig. 2 is that R is even more variable than shown in Fig. 1. On an annual basis, the domain-averaged values of R are 1.38 and 1.06 for tropical and extratropical regions, respectively. The summer and winter histograms in Fig. 2 suggest that R depends on season more in the extratropical regions than in the tropics. A common feature of all the histograms is a sizeable fraction of months with $R<1$. This may be explained by the abundance of cirriform clouds in many locations[27]. As these clouds are high, photons are less likely to be absorbed by low-level cloud, aerosol and water vapour (Table 1). Also worth noting is the considerable fraction of cases in the tropics with extremely large values of R (>3). These values of R are barely meaningful, as almost 50% of them occurred when $|CRF_{TOA}| < 5$ W m^{-2}. Furthermore, small errors in CRF_{TOA} could lead to enormous values of R when $|CRF_{TOA}|$ is near zero. Therefore, R in these cases is not significant when assessing the effect of clouds on atmospheric absorption of solar radiation.

Figure 3 shows 94 monthly values of R for three German cells, each of which contained at least seven pyranometers (match-up errors less than 4 W m^{-2}). The seasonality of R is apparent, with smallest and largest values in the winter and summer respectively. Also, the interannual variability of R is striking: variations of 0.2–0.3 are common. The curves in Fig. 3 represent R as simulated by the model used to produce Table 1 for two extreme cloud conditions which favour low and high values of R. Comparing measured R to calculated R suggests that this ratio is much affected by changing distributions of both solar zenith angle (seasonal) and cloud conditions (seasonal and interannual). As the theoretical curves envelop about 85% of the observed values, this may indicate that for mid-latitudes the effect of clouds on total atmospheric absorption is within the reach of conventional radiation models, although discrepancies of smaller magnitude between models and observations are still entirely possible. Considering, however, that the upper envelope in Fig. 3 corresponds to an extreme condition that rarely exists,

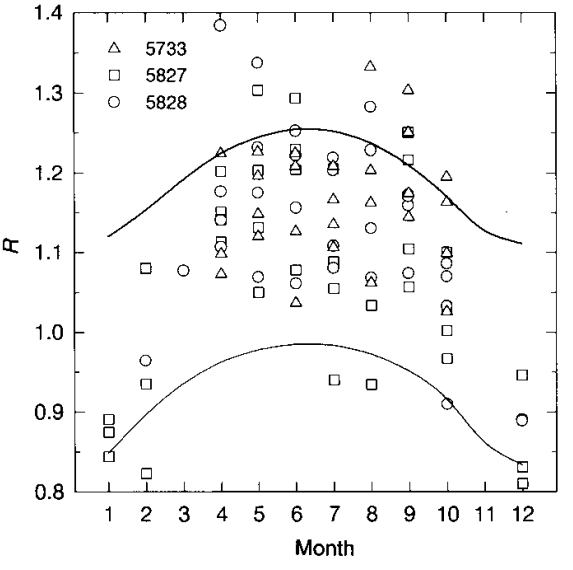

FIG. 3 Intra- and inter-annual variations of R for three German cells denoted by their serial numbers. Latitudes and longitudes at the centres of the cells are 51° 15′ N, 2° E for 5827; 51° 15′ N, 10° E for 5828; and 48° 45′ N, 9° 28′ E for 5733. The curves denote model-simulated diurnal-mean R for conditions favouring extremely low and high values of R. The thick (upper) curve represents a mid-latitude summer atmosphere with continental aerosol of optical depth 0.45 and cumulus cloud[14] of optical depth 40 situated between 0 and 1 km height. The thin (lower) curve corresponds to an aerosol-free, subarctic winter atmosphere with a St-I[14] cloud of optical depth 40 situated between 9 and 13 km height. Land surface at 50° N was used in the calculation of these two curves.

TABLE 1 Sensitivities of R to various factors

Surface	Cloud type	Cloud location (km)	R
Sensitivity to surface type			
Desert	St-I	2–4	0.94
Snow	St-I	2–4	0.64
Water	St-I	2–4	1.03
Crop	St-I	2–4	0.97
Sensitivity to cloud type			
Crop	St-I	2–4	0.97
Crop	Cb	2–4	1.07
Crop	Cu	2–4	1.01
Crop	Sc-II	2–4	1.00
Sensitivity to height of cloud top			
Crop	St-I	0–1	1.17
Crop	St-I	0–2	1.09
Crop	St-I	0–4	1.02
Crop	St-I	0–6	0.98
Crop	St-I	0–9	0.93
Crop	St-I	0–13	0.88
Sensitivity to cloud height			
Crop	St-I	2–4	0.97
Crop	St-I	6–9	0.86

These values of diurnal-mean R were calculated (for 30° N in July) by a doubling-adding code which contained 429 spectral intervals and 8 vertical layers. It accounted for multiple Rayleigh and Mie scattering, and absorption by gases, aerosol and cloud droplets. Henyey–Greenstein phase functions were used. Mid-latitude summer atmosphere[33] conditions, with continental aerosol of optical depth 0.225 at 550 nm wavelength, were employed. Surface broadband albedos for snow, desert, crop and water of 0.91, 0.40, 0.27 and 0.08, respectively, were used. Cloud optical depth was 40 and the size distributions of cloud droplets for four cloud types (stratus (St-I), cumulonimbus (Cb), cumulus (Cu) and stratocumulus (Sc-II)) were as defined in ref. 14.

values of R near and exceeding it represent cases which are beyond these models.

The data used to produce Fig. 3 were also employed to derive R by the regression technique used by Cess *et al.*[4]. These data have the least uncertainties owing to the high density of pyranometers and homogeneous surface types. Figure 4 shows a strong linear relationship between monthly-mean TOA albedo and atmospheric transmittance. The slope of the regression line s is

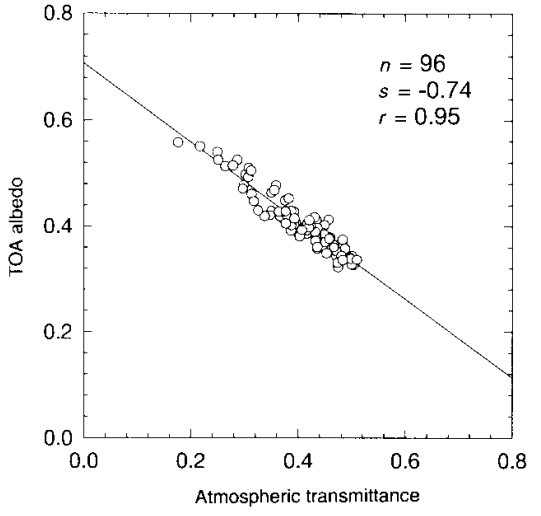

FIG. 4 Scatter plot of monthly-mean TOA albedo measured by ERBE verses monthly-mean atmospheric transmittance determined from surface insolation measurements for the cells used in Fig. 3. n denotes the number of samples, s and r are respectively the slope and correlation coefficient of the linear regression.

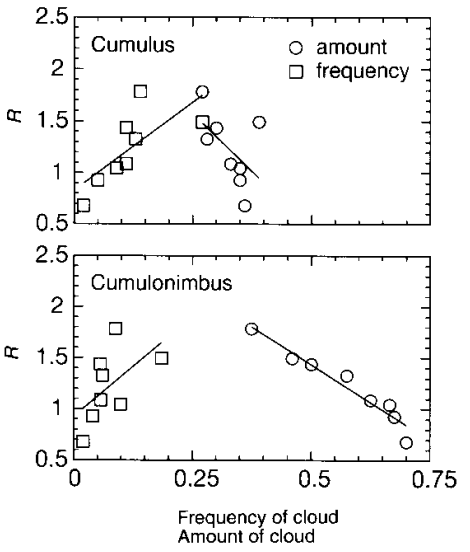

FIG. 5 Annual, zonal-mean values of R in the Northern Hemisphere as a function of corresponding frequency of occurrence and amount (when present) of cumulus (top panel) and cumulonimbus (bottom panel) clouds[31]. Straight lines are least-square, linear-regression fits to the data. Only the slopes with respect to frequency for cumulus, and with respect to amount for cumulonimbus, are significantly different from zero at the 90% confidence level.

-0.74 ± 0.06 (at 95% confidence level) which is slightly less than values generated using GCM data[4]. The mean surface albedo for this region was estimated[18,20] to be 0.15. Thus the corresponding value of R calculated from equation (4) is 1.15 which coincides well with that derived from the CRFs for the same region. Analyses were also made for 11 individual cells having at least three pyranometers. Slopes were found to vary from -0.67 to -0.87 with a mean of -0.77 with correlation coefficients generally larger than 0.9. The disagreement between our estimate of R for the extratropics, and those of Cess *et al.*[4] is therefore not due to different analytical methods, but, rather, different data sets (and possibly different averaging periods).

So far, the observed variation of R has been explained by changes in solar zenith angle and aerosol effects. The potential dependence of R on cloud structure also deserves examination. Clouds that most affect the TOA solar radiation budget are cumuliform in the tropics and stratiform in the extratropics[28]. Thus, it seems reasonable to hypothesize that latitudinal variations in R may be associated partly with differing radiative transfer characteristics stemming from differences in cloud morphology[29,30]. Figure 5 shows a plot of annual zonal-mean R versus corresponding frequencies of occurrence (fraction of time when clouds are present) and amount (fraction of the sky covered by cloud when they are present) of cumulus (Cu) and cumulonimbus (Cb) clouds[31]. In both cases, R tends to increase as frequency increases and as amount decreases. Hence, it may be tempting to infer from Fig. 5 that enhanced values of R are associated with convective clouds. However, Monte Carlo photon-transport experiments with four spectral bands[32] for a variety of towering three-dimensional cloud fields (pure water) in the standard tropical atmosphere[33] yielded diurnal-mean values of R that exceeded their plane-parallel counterpart by no more than 0.15. Moreover, inclusion of reduced single-scattering albedos for large droplets[31], as characteristic of convective clouds, did not yield significantly larger values of R, but merely enhanced absorption by droplets at the expense of reduced absorption by water vapour in the lower troposphere.

Concluding remarks

In terms of magnitude, estimates of R from this work are not inconsistent with those of recent studies[4–6] for the tropics, but are at variance with those for other regions[4]. The apparent agree-

ment in the tropics should be treated with scepticism given the potential effects of biomass burning aerosols and large uncertainties in the satellite and ground-based data. Such strongly absorbing aerosols not only increase cloud absorption—and thus the value of R—but also lead to an overestimation of R. This is because the clear-sky surface net solar flux is probably overestimated by the inversion algorithm[15] which only incorporates a small amount of weakly absorbing aerosol. Larger uncertainties of R for the tropics also stem from too-small data samples due to lower pyranometer density and shorter duration of measurements, and too-noisy data associated with the relatively small amounts of thick cloud. In view of these problems, we have much less confidence on the larger values of R found in the tropics than the smaller values of R in the mid-latitudes. Until these problems are resolved, one cannot attribute unambiguously the large values of R to the cloud absorption anomaly. As the discrepancy with ref. 4 for the extratropics is largely related to the use of different data sets, rather than to different analytical methods, it is imperative that the data sets involved undergo detailed intercomparisons. Such an analysis should enable the evaluation of whether a substantial revision of our present understanding of the atmosphere's energy budget resulting from the treatment of cloud absorption as indicated by Cess *et al.* is required.

We note that this study does not rule out the existence of the cloud absorption anomaly, but rather indicates that its magnitude (if it exists) on a global scale may not be as large as suggested in some recent reports. If so, the use of R may not be an effective means of addressing the cloud absorption anomaly. R is not a direct measure of cloud absorption, as its value is influenced by many factors other than clouds. □

Received 10 March; accepted 17 July 1995.

1. Cess, R. D. *et al. Science* **245,** 513–516 (1989).
2. Stephens, G. L. & Tsay, S.-C. *Q. Jl R. met. Soc.* **116,** 671–704 (1990).
3. Hayasaka, T., Kikuchi, N. & Tanaka, M. *J. appl. Met.* **34,** 1047–1055 (1995).
4. Cess, R. D. *et al. Science* **267,** 496–499 (1995).
5. Ramanathan, V. *et al. Science* **267,** 499–503 (1995).
6. Pilewskie, P. & Valero, F. P. *Science* **267,** 1626–1629 (1995).
7. Chou, M.-D., Arking, A., Otterman, J. & Ridgway, W. L. *Geophys. Res. Lett.* **22,** 1885–1888 (1995).
8. Li, Z. & Barker, H. *World Met. Org. TD-No.* **648,** 110–113 (Geneva, 1994).
9. Barker, H. & Li, Z. *J. Clim.* **8,** 2213–2223 (1995).
10. Zhang, M.-H., Cess, R. D., Kwon, T. Y. & Chen, M. H. *J. geophys. Res.* **99,** 5515–5523 (1994).
11. Barker, H. W. *J. geophys. Res.* **100,** 1017–1025 (1995).
12. Ramanathan, V. *et al. Science* **243,** 57–63 (1989).
13. Li, Z., Leighton, H. G., Takashima, T. & Masuda, K. *J. Clim.* **6,** 317–330 (1993).
14. Stephens, G. L. *J. atmos. Sci.* **35,** 2111–2122 (1978).
15. Barkstrom, B. *et al. Bull. Am. met. Soc.* **70,** 1254–1262 (1989).
16. Ohmura, A. & Gilgen, H. *Global Energy Balance Archive* (Zurcher Geogra. Schriften, Heft 44, Fachvereine, Zurich, 1991).
17. Whitlock, C. H. Tech. Memo. 107747 (NASA, Hampton, VA, 1990).
18. Darnell, W. L., Staylor, W. F., Gupta, S. K., Ritchey, N. A. & Wilber, A. C. *J. geophys. Res.* **97,** 15741–15760 (1992).
19. Li, Z., Leighton, H. G. & Cess, R. D. *J. Clim.* **6,** 1764–1772 (1993).
20. Li, Z. & Garand, L. *J. geophys. Res.* **99,** 8335–8351 (1994).
21. Li, Z., Whitlock, C. H. & Charlock, T. P. *J. Clim.* **8,** 315–328 (1995).
22. Crutzen, P. J. & Andreae, O. M. *Science* **250,** 1669–1678 (1990).
23. Cahoon, D. R. Jr, Stocks, B. J., Levine, J. S., Cofer, W. R. & O'Neill, K. P. *Nature* **359,** 812–815 (1992).
24. Kaufman, Y. J. *et al. J. geophys. Res.* **97,** 14581–14599 (1992).
25. Langner, J. & Rodhe, H. *J. atmos. Chem.* **13,** 225–263 (1991).
26. Blanchet, J.-P., Heintzenberg, J. & Winkler, P. *Contemp. atmos. Phys.* **54,** 143–158 (1986).
27. Wylie, D. P., Menzel, W. P., Woolf, H. M. & Strabala, K. I. *J. Clim.* **7,** 1972–1986 (1994).
28. Okert-Bell, M. E. & Hartmann, D. L. *J. Clim.* **5,** 1157–1171 (1992).
29. Davies, R. *J. atmos. Sci.* **35,** 1712–1725 (1978).
30. Barker, H. W. & Davies, J. A. *J. atmos. Sci.* **49,** 1115–1126 (1992).
31. Warren, S. G., Hahn, C. J., London, J., Chervin, R. M. & Jenne, R. L. Tech. note NCAR/TN-273+STR (National Center for Atmospheric Research, Boulder, CO, 1986).
32. Slingo, A. *J. atmos. Sci.* **46,** 1419–1427 (1989).
33. McClatchey, R. A., Fenn, R. W., Selby, J. E. A., Volz, F. E. & Garing, J. S. Report No. AFCRL-71-0279 (US Air Force Cambridge Res. Lab., Cambridge, MA, 1971).
34. Wiscombe, W. J., Welch, R. M. & Hall, W. D. *J. atmos. Sci.* **41,** 1336–1355 (1984).